To investigate the localization of dendrin in injured podocytes, immunostaining and WB analyses were performed using ADR-induced nephrotic kidneys. The expression pattern of dendrin showed a dotted pattern in glomeruli on days 7 and 15. An accumulation of dendrin was found in the podocyte nuclei, especially on day 3 after ADR injection. The expression of dendrin was almost restored on day 28 (**Figure 4A**). In the WB analysis for dendrin with GAPDH as the internal control, the expression of dendrin started to decrease on day 7. The expression was restored on day 28 (**Figure 4B**). In immunostaining with the nuclear podocyte marker WT-1 and dendrin, an accumulation of dendrin in the podocyte nuclei was found on day 3 after ADR injection (**Figure 4C**). Double-positive cells of dendrin and WT1 were counted in each period. A number of dendrin-positive nuclei were detected from day 3. On day 3 after ADR injection, the number of nuclear dendrin-positive podocytes (WT-1 positive cells) increased significantly compared to the number in the controls (% dendrin positive nuclei number / WT-1 positive cell number of controls versus day 3 in glomerulus :12.9 ± 1.9 vs, 23.4 ± 2.2, $p< 0.01$ versus control, each 30 glomeruli in n=3) (**Figure 4D**). To test whether ADR directly induced relocation of dendrin to the nuclei, the number of dendrin-positive nuclei in cultured podocytes was counted after 6 hours of incubation with ADR. The number of dendrin-positive nuclei in podocytes injured by ADR was significantly increased compared with control podocytes (%; nuclear control dendrin versus dendrin in podocytes injured by ADR: 8.81 ± 0.90 vs,

26.20 ± 3.23, p=0.001, assessed with 2000 cells, n=3) (**Figure 5A, B**).

Nuclear dendrin was detected in several human glomerular diseases, but not in MCD.

To examine the presence of translocated dendrin to podocyte nuclei in human glomerular diseases, we produced anti-human dendrin antibody and did immunostaining of dendrin on human kidney biopsy specimens. Anti-human dendrin antibody was designed to detect not only human dendrin, but also rat dendrin. Using WB analyses, the expression of dendrin was clearly detected in human and rat dendrin over-expressing HEK cells and in isolated rat glomeruli, but not in whole kidneys (**Supplementary Figure 1A, B**). After immunostaining, a linear pattern of dendrin was detected in normal rat kidneys (**Supplementary Figure 1C**). The staining pattern of dendrin almost merged with that of synaptopodin, but not with that of podocalyxin, because podocalyxin was located on the podocyte cell body and on primary FPs. Triple staining of human glomerulopathy with dendrin, podcalyxin and DAPI was then performed. Podocalyxin staining was used to detect the nuclear localization of dendrin, because the podocyte nucleus should be detected within the podocalyxin positive area. In MCD, dendrin staining showed both linear and dotted patterns in the capillary area (**Figure 6A**). Some dendrin-positive nuclei in glomeruli were detected in biopsy specimens from FSGS (**Figure 6B**). Dendrin-positive nuclei

in the glomeruli were also detected in specimens from LN (**Figure 6C**) and MN (**Figure 6D**). The mean number of dendrin-positive nuclei per glomerulus were (1.60 ± 0.51, 1.00 ± 0.58, 11.25 ±2.78, 6.33 ±0.67 and 13.00 ± 4.95 in samples from control kidney biopsy specimens (n=5), MCD (n=3), FSGS (n=3), MN (n=3) and LN (n=4), respectively (Figure7). Samples in FSGS, MN and LN, showed significantly higher numbers of dendrin-positive nuclei per glomerulus than control samples ($p<0.05$).

Discussion:

Guo et al. showed that ADR induces transcripts of TGF-β1 and connective tissue growth factor and production of AGE and reactive oxygen species (ROS) 3 days after ADR injection in mice [29]. Koshikawa et al. also showed there was a marked increase in phosphorylated p38 MAPK in the podocytes of ADR nephropathy on day 3 [30]. In the present study, apoptotic cells increased the most and foot-process effacements in glomeruli were detected on day 3, when urinary albumin excretion was still within a normal range. Interestingly, a significantly higher number of dendrin-positive podocyte nuclei were detected on day 3 after ADR injection in mice. Furthermore, a 6-hr treatment with ADR, not inducing podocyte apoptosis, promoted relocation of dendrin to the nuclei of cultured podocytes. It is conceivable that some intracellular signaling cascades will give rise to serial reactions of the genes and proteins, including dendrin, that alter barrier function and cause podocyte apoptosis leading to overt proteinuria and podocyte loss.

To detect podocyte nuclei in mouse kidneys, anti-WT-1 antibody is usually used. However, the mouse monoclonal WT-1 antibody that gave a cytoplasmic stain of human glomeruli was not used, as Murea et al. reported [31]. Instead, anti-podocalyxin antibody and DAPI staining to detect podocyte nuclei in human kidney biopsy specimens was used in the present study.

Some reports suggest that podocyte apoptosis causes podocyte loss and leads to

glomerulosclerosis in human glomerulopathy [9,12]. In MCD, there was no podocyte loss and glomerulosclerosis [1]. Duner et al. reported that nuclear dendrin was not detected in MCD, although dendrin are re-distributed within podocytes [21]. In the present study, most dendrin was located at the SD area in MCD. However, it was possible to detect dendrin clearly located to the podocyte nucleus in FSGS, MN and LN. Podocyte apoptosis has reportedly caused podocyte loss and led to glomerulosclerosis [1]. These results suggest that relocation of dendrin to the podocyte nucleus as a response to injury might be related to podocyte apoptosis and the loss of podocytes from the GBM in human glomerulopathy, but not in MCD. The amount of nuclear dendrin could be an indicator of disease activity and progression to glomerulosclerosis and end stage renal disease (ESRD) in renal biopsy. In future studies, it will be necessary to investigate the relationship between nuclear dendrin and disease progression and activity in human glomerular disease.

The SD represents a signaling platform that contributes to the regulation of podocyte function in health and disease [32]. Both CD2AP and nephrin, SD-associated proteins, interact with the p85 regulatory subunit of phosphatidylinositol 3-kinase *in vivo*, stimulating antiapoptotic Akt signaling [2,33,34]. Podocytes lacking CD2AP are more susceptible to apoptosis, and mice lacking CD2AP show increased podocyte apoptosis [4,35]. Reportedly, the C-terminus of dendrin interacts with CD2AP [20]. Thus, it is possible that CD2AP regulates localization and nuclear translocation of

dendrin in injured podocytes. However, it is still unknown how nuclear dendrin provokes apoptosis in injured podocytes. Now, we are trying to elucidate how nuclear dendrin helps to promote podocyte apoptosis.

This study demonstrated that severe podocyte injury, which ADR causes in mice, induced translocation of dendrin to the podocyte nucleus before urinary albumin excretion, and podocyte loss and glomerulosclerosis developed. Moreover, nuclear dendrin was found in patients with glomerulopathies (FSGS, MN and LN), but not in MCD. These results suggest that the location of dendrin in the nucleus is a candidate novel marker to estimate the number of podocyte loss and to predict progression to glomerulosclerosis.

Acknowledgments

We thank Prof. Peter Mundel (University of Miami, Miller School of Medicine) for helpful discussions; Dr. Yutaka Kanamaru (Juntendo University) for his technical assistance and helpful discussions; and, Ms. Kaori Takahashi, Mr. Junichi Nakamoto, Mr. Mitsutaka Yoshida and Mr. Alehandro Oliva (Juntendo University) for their excellent technical assistance. This work was supported by research grants from the Takeda Science Foundation, Kanae Foundation for the Promotion of Medical Science and Kowa Life Science Foundation to K.A.; by a Grant–in-Aid for Scientific Research (Grant-in–Aid for Young Scientists (Start-up): (19890213) to K.A.; by Challenging Exploratory Research:(21659217) to K.A.; by a Grant-in–Aid for Young Scientists (B):(21790821) to E.A.; by a projected research grant from Juntendo University to MT; by a grant-in-aid (No. 12146205) to E.K for Scientific Research, by a grant-in-aid (No. 18076005) to T.U. for Scientific Research on Priority Areas from the Ministry of Education, Science, Sports and Culture of Japan, and by a grant-in-aid for the Third-Term Comprehensive 10-Year Strategy for Cancer Control from the Ministry of Health, Labor and Welfare (No. 16271401) to T.U.

Figure legends

Figure 1: ADR induced nephrosis and caused glomerulosclerosis in mice.

A single dose (11 mg/ kg BW) of ADR was injected via the tail vein to achieve a nephrotic state. Urine samples were collected from all mice once every few days. (**A**) ADR induced massive albuminuria (ACR: urinary albumin creatinine ratio), with two significant peaks on days 7 and 28 (n=5-10, P< 0.01). The columns represent the mean ± SE of each value from different samples. Asterisks show that the difference in the urinary albumin creatinine ratio, from that on day 0, was significant. (**B**) Partial glomerulosclerosis was observed from day 7 and gradually increased. At day 28 after ADR injection, there were many casts and wide-ranging glomerulosclerosis compared with the control. Original magnifications were x 100 (for lower magnification) and x 400 (for higher magnification). (**C**) The incidence of sclerotic glomeruli among the total glomeruli per section on day 28 after ADR injection showed a significantly higher rate than that on day 0 (each 100 glomeruli in n=3, p< 0.05). Asterisks show that the difference in the sclerotic glomerulus/total glomerulus ratio, compared with day 0, was significant. (**D**) There was a significant increase in GB ratio between day 0 and day 28 after ADR injection (n=3, p< 0.05). Asterisks show that the difference in the GB ratio compared with day 0 was significant. The columns represent the mean ± SE of each value from different samples. (E) Kidneys with ADR-induced nephropathy showed FP effacement by EM. There was no FP effacement in the control glomerulus. FP

effacement (**arrows**) was observed from day 3 and was markedly increased from day 7 to day 28. Original magnifications were x 3,000 and x 10,000, Scale bar, 5μm.

Figure 2: Injection of ADR caused loss of podocytes in mice.

(**A, B**) Mean podocyte numbers per glomerulus in the controls and on day 28 are shown for both DAPI positive and WT-1 positive cells (**asterisks**). Original magnification was x 1,000. (**C**) A significant decrease in the number of podocytes was detected on day 28. After triple staining with WT-1, synaptopodin and DAPI, WT-1-positive cells on day 28 were significantly lower than the control level (each 50 glomeruli in n=3, $P< 0.01$). The columns represent the mean ± SE of each value from different samples.

Figure 3: ADR induces podocyte apoptosis *in vivo* and *in vitro*.

(**A**) TUNEL-positive cells in glomeruli (**B**) showed the highest numbers on day 3. Asterisks show that the difference in the TUNEL positive cells/total glomerulus compared with day 0 is significant. The columns represent the mean ± SE of each value from different samples (n=3, $p< 0.05$). (**C**) Analysis of hypoploid nuclei in cultured differentiated podocytes after treatment with 0.01 μg/ml to 1.0 μg/ml of ADR or control for 48 hours. Treatment with 0.25 μg/ml to 1.0 μg/ml of ADR induced significant apoptosis (n=3, $P<0.0001$). (**D**) Analysis of hypoploid nuclei after treatment

with 0.25 μg/ml of ADR for 24, 48 and 72 hours and control. Treatment with ADR for 48 and 72 hours induced significant apoptosis (n=3, $p<0.0001$). Asterisks show that the difference in the percentage (apoptotic cells/all cells) compared with the controls was significant. The columns represent the mean ± SE of each value from different samples. (**E, F**) Analysis of annexin V/PI double-positive populations in cultured differentiated podocytes after treatment with 0.25 μg/ml of ADR for 24 and 48 hours. This method also showed that treatment with ADR for 48 hours induced significant podocyte apoptosis (n=3, $p<0.0001$). Annexin V-positive cells (PI-negative), PI-positive cells (Annexin V-negative) and double-positive cells indicate early apoptotic cells, necrotic cells and late apoptotic cells, respectively. Asterisks show the differences from the controls in the percentage of late apoptosis/all cells, early apoptosis/all cells and whole apoptosis/all cells, which were significant. The columns represent the mean ± SE of each value from different samples. (**G**) To evaluate the expression of cleaved caspase-3, cells were treated with ADR (0.25 μg/ ml) for 0, 3 and 6 hours. The expression increased at 6 hours after ADR treatment per WB analysis. (H) The localization of cleaved caspase-3 in ADR-injected kidneys (day3) was investigated by immunostaining.

Figure 4: Expression and localization of dendrin in ADR-injected mice.

(**A**) The expression and localization of dendrin in control and ADR-injected kidneys

(days 3, 7, 15 and 28) were investigated by immunostaining. Significant nuclear localization of dendrin in podocytes (asterisks) was detected on day 3. Original magnification was x 1,000. **(B)** In the WB for dendrin and GAPDH, reduction of dendrin due to ADR nephropathy was observed on days 7 and 15, whereas GAPDH showed no reduction. **(C)** To count the number of dendrin positive-nuclei in podocytes, double staining of dendrin and WT1 was performed. The nuclear localization of dendrin (asterisks) in podocytes was significant on day 3. **(D)** The numbers of dendrin-positive nuclei and WT-1-positive nuclei per glomerulus were significant on day 3 (30 glomeruli each in n=3, $P< 0.05$). Asterisks show that the difference in the ratio, compared with the controls, was significant. The columns represent the mean ± SE of each value from different samples.

Figure 5: ADR induced nuclear import of dendrin in cultured podocytes.

(A) ADR induced nuclear import of dendrin after serum starvation for 24 hours. Nuclear translocation of dendrin can be completed in 6 hours. **(B)** Quantitative analysis of ADR-induced nuclear import of dendrin. For details, see ***Results***.

Figure 6: Kidney sections from several human glomerulopathies showed the nuclear relocation of dendrin.

(**A- D**) To show nuclear dendrin in human glomerular diseases, triple staining for

dendrin, podocalyxin and DAPI was performed. Nuclear dendrin was shown as an image surrounded by podocalyxin and merged with DAPI. There were some clear dendrin-positive nuclei in FSGS (**C**), MN (**F**) and LN (**E**). On the other hand, few dendrin-positive nuclei were present in MCD (**A**). Original magnification was ×400 (for lower magnification), ×1,000 (for higher magnification).

Figure 7: Glomerular expression of nuclear dendrin in several glomerular diseases. The numbers of dendrin-positive nuclei per glomerulus were statistically significant for FSGS, MN and LN. Asterisks show that the difference in the ratio, compared with the controls, was significant ($p<0.05$). The columns represent the mean ± SE of each value from different samples.

References

[1] Mundel P, Shankland SJ: Podocyte biology and response to injury. J Am Soc Nephrol 2002;13:3005-3015.

[2] Somlo S, Mundel P: Getting a foothold in nephrotic syndrome. Nat Genet 2000;24:333-335.

[3] Faul C, Donnelly M, Merscher-Gomez S, Chang YH, Franz S, Delfgaauw J, Chang JM, Choi HY, Campbell KN, Kim K, Reiser J, Mundel P: The actin cytoskeleton of kidney podocytes is a direct target of the antiproteinuric effect of cyclosporine A. Nat Med 2008;14:931-938.

[4] Shankland SJ: The podocyte's response to injury: role in proteinuria and glomerulosclerosis. Kidney Int 2006;69:2131-2147.

[5] Kriz W, LeHir M: Pathways to nephron loss starting from glomerular diseases-insights from animal models. Kidney Int 2005;67:404-419.

[6] Wang W, Tzanidis A, Divjak M, Thomson NM, Stein-Oakley AN: Altered signaling and regulatory mechanisms of apoptosis in focal and segmental glomerulosclerosis. J Am Soc Nephrol 2001;12:1422-1433.

[7] Caulfield JP, Reid JJ, Farquhar MG: Alterations of the glomerular epithelium in acute aminonucleoside nephrosis. Evidence for formation of occluding junctions and epithelial cell detachment. Lab Invest 1976;34:43-59.

[8] Inokuchi S, Shirato I, Kobayashi N, Koide H, Tomino Y, Sakai T: Re-evaluation of foot process effacement in acute puromycin aminonucleoside nephrosis. Kidney Int 1996;50:1278-1287.

[9] Hishiki T, Shirato I, Takahashi Y, Funabiki K, Horikoshi S, Tomino Y: Podocyte injury predicts prognosis in patients with iga nephropathy using a small amount of renal biopsy tissue. Kidney Blood Press Res 2001;24:99-104.

[10] Pagtalunan ME, Miller PL, Jumping-Eagle S, Nelson RG, Myers BD, Rennke HG, Coplon NS, Sun L, Meyer TW: Podocyte loss and progressive glomerular injury in type II diabetes. J Clin Invest 1997;99:342-348.

[11] Kim YH, Goyal M, Kurnit D, Wharram B, Wiggins J, Holzman L, Kershaw D, Wiggins R: Podocyte depletion and glomerulosclerosis have a direct relationship in the PAN-treated rat. Kidney Int 2001;60:957-968.

[12] Lemley KV: Diabetes and chronic kidney disease: lessons from the Pima Indians. Pediatr Nephrol 2008;23:1933-1940.

[13] Lemley KV, Lafayette RA, Safai M, Derby G, Blouch K, Squarer A, Myers BD: Podocytopenia and disease severity in IgA nephropathy. Kidney Int 2002;61:1475-1485.

[14] Bertani T, Poggi A, Pozzoni R, Delaini F, Sacchi G, Thoua Y, Mecca G, Remuzzi G, Donati MB: Adriamycin-induced nephrotic syndrome in rats: sequence of pathologic events. Lab Invest 1982;46:16-23.

[15] Nakhoul F, Ramadan R, Khankin E, Yaccob A, Kositch Z, Lewin M, Assady S, Abassi Z: Glomerular abundance of nephrin and podocin in experimental nephrotic syndrome: different effects of antiproteinuric therapies. Am J Physiol Renal Physiol 2005;289:F880-90.

[16] Reiser J, von Gersdorff G, Loos M, Oh J, Asanuma K, Giardino L, Rastaldi MP, Calvaresi N, Watanabe H, Schwarz K, Faul C, Kretzler M, Davidson A, Sugimoto H, Kalluri R, Sharpe AH, Kreidberg JA, Mundel P: Induction of B7-1 in podocytes is associated with nephrotic syndrome. J Clin Invest 2004;113:1390-1397.

[17] Chen A, Sheu LF, Ho YS, Lin YF, Chou WY, Chou TC, Lee WH: Experimental focal segmental glomerulosclerosis in mice. Nephron 1998;78:440-452.

[18] Lee VW, Harris DC: Adriamycin nephropathy: a model of focal segmental glomerulosclerosis. Nephrology (Carlton) 2011;16:30-38.

[19] Neuner-Jehle M, Denizot JP, Borbely AA, Mallet J: Characterization and sleep deprivation-induced expression modulation of dendrin, a novel dendritic protein in rat brain neurons. J Neurosci Res 1996;46:138-151.

[20] Asanuma K, Campbell KN, Kim K, Faul C, Mundel P: Nuclear relocation of the nephrin and CD2AP-binding protein dendrin promotes apoptosis of podocytes. Proc Natl Acad Sci U S A 2007;104:10134-10139.

[21] Duner F, Patrakka J, Xiao Z, Larsson J, Vlamis-Gardikas A, Pettersson E, Tryggvason K, Hultenby K, Wernerson A: Dendrin expression in glomerulogenesis

and in human minimal change nephrotic syndrome. Nephrol Dial Transplant 2008;23:2504-2511.

[22] Tanimoto M, Gohda T, Kaneko S, Hagiwara S, Murakoshi M, Aoki T, Yamada K, Ito T, Matsumoto M, Horikoshi S, Tomino Y: Effect of pyridoxamine (K-163), an inhibitor of advanced glycation end products, on type 2 diabetic nephropathy in KK-A(y)/Ta mice. Metabolism 2007;56:160-167.

[23] Asanuma K, Kim K, Oh J, Giardino L, Chabanis S, Faul C, Reiser J, Mundel P: Synaptopodin regulates the actin-bundling activity of alpha-actinin in an isoform-specific manner. J Clin Invest 2005;115:1188-1198.

[24] Tanimoto M, Fan Q, Gohda T, Shike T, Makita Y, Tomino Y: Effect of pioglitazone on the early stage of type 2 diabetic nephropathy in KK/Ta mice. Metabolism 2004;53:1473-1479.

[25] Asanuma K, Tanida I, Shirato I, Ueno T, Takahara H, Nishitani T, Kominami E, Tomino Y: MAP-LC3, a promising autophagosomal marker, is processed during the differentiation and recovery of podocytes from PAN nephrosis. FASEB J 2003;17:1165-1167.

[26] Kanamaru Y, Tamouza H, Pfirsch S, El-Mehdi D, Guerin-Marchand C, Pretolani M, Blank U, Monteiro RC: IgA Fc receptor I signals apoptosis through the FcRgamma ITAM and affects tumor growth. Blood 2007;109:203-211.

[27] Luimula P, Ahola H, Wang SX, Solin ML, Aaltonen P, Tikkanen I, Kerjaschki D, Holthofer H: Nephrin in experimental glomerular disease. Kidney Int 2000;58:1461-1468.

[28] Kawachi H, Koike H, Kurihara H, Sakai T, Shimizu F: Cloning of rat homologue of podocin: expression in proteinuric states and in developing glomeruli. J Am Soc Nephrol 2003;14:46-56.

[29] Guo J, Ananthakrishnan R, Qu W, Lu Y, Reiniger N, Zeng S, Ma W, Rosario R, Yan SF, Ramasamy R, D'Agati V, Schmidt AM: RAGE mediates podocyte injury in adriamycin-induced glomerulosclerosis. J Am Soc Nephrol 2008;19:961-972.

[30] Koshikawa M, Mukoyama M, Mori K, Suganami T, Sawai K, Yoshioka T, Nagae T, Yokoi H, Kawachi H, Shimizu F, Sugawara A, Nakao K: Role of p38 mitogen-activated protein kinase activation in podocyte injury and proteinuria in experimental nephrotic syndrome. J Am Soc Nephrol 2005;16:2690-2701.

[31] Murea M, Park JK, Sharma S, Kato H, Gruenwald A, Niranjan T, Si H, Thomas DB, Pullman JM, Melamed ML, Susztak K: Expression of Notch pathway proteins correlates with albuminuria, glomerulosclerosis, and renal function. Kidney Int 2010;78:514-522.

[32] Faul C, Asanuma K, Yanagida-Asanuma E, Kim K, Mundel P: Actin up: regulation of podocyte structure and function by components of the actin cytoskeleton. Trends Cell Biol 2007;17:428-437.

[33] Benzing T: Signaling at the slit diaphragm. J Am Soc Nephrol 2004;15:1382-1391.

[34] Huber TB, Hartleben B, Kim J, Schmidts M, Schermer B, Keil A, Egger L, Lecha RL, Borner C, Pavenstadt H, Shaw AS, Walz G, Benzing T: Nephrin and CD2AP associate with phosphoinositide 3-OH kinase and stimulate AKT-dependent signaling. Mol Cell Biol 2003;23:4917-4928.

[35] Schiffer M, Mundel P, Shaw AS, Bottinger EP: A novel role for the adaptor molecule CD2-associated protein in transforming growth factor-beta-induced apoptosis. J Biol Chem 2004;279:37004-37012.

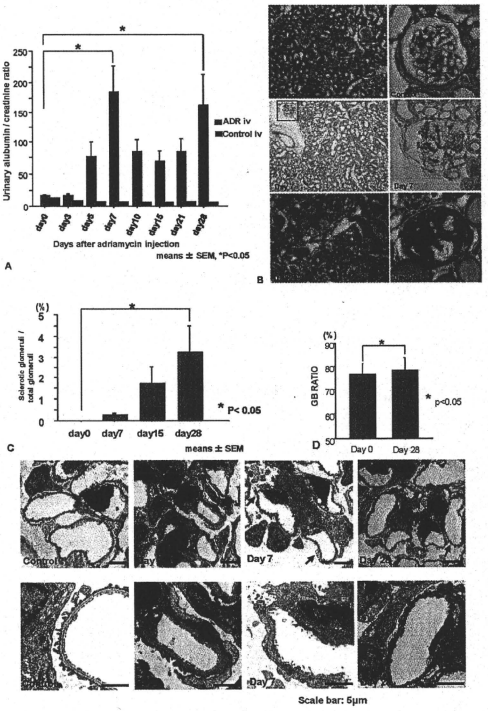

Figure 1

170x245mm (220 x 220 DPI)

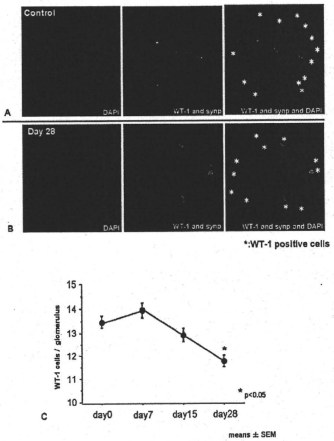

Figure 2

170x245mm (258 x 282 DPI)

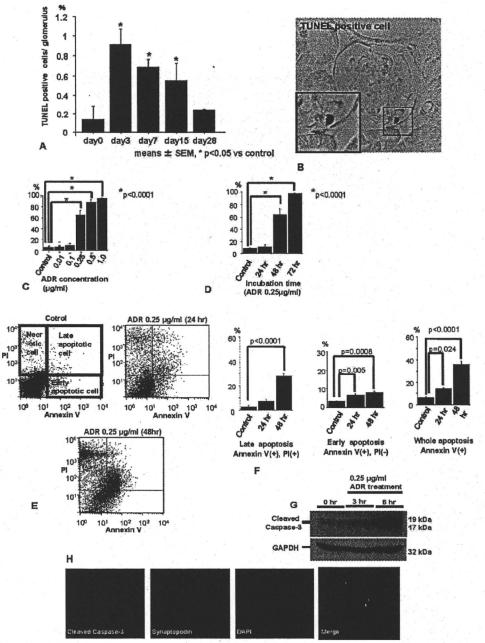

Figure 3

170x245mm (220 x 220 DPI)

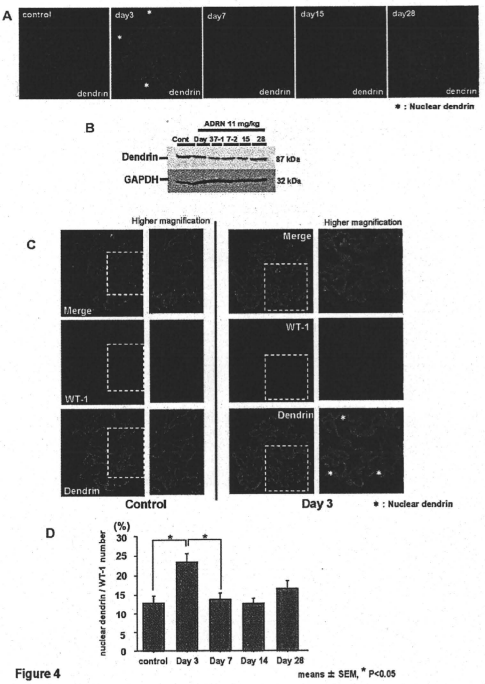

Figure 4

170x245mm (219 x 220 DPI)